Available online at www.sciencedirect.com
SCIENCE DIRECT®
International Journal of Mass Spectrometry 236 (2004) 81–90
International Journal of Mass Spectrometry
www.elsevier.com/locate/ijms

# Hydration of protonated primary amines: effects of intermolecular and intramolecular hydrogen bonds

Dengfeng Liu, Thomas Wyttenbach, Michael T. Bowers*

*Department of Chemistry and Biochemistry, University of California at Santa Barbara, Santa Barbara, CA 93106, USA*

Received 14 April 2004; accepted 31 May 2004

Available online 20 July 2004

**Abstract**

Addition of individual water molecules to a number of protonated primary amines, $RNH_3^+$, was studied experimentally by measuring hydration equilibria in a mass spectrometer equipped with an ion mobility cell and theoretically using molecular mechanics and density functional theory calculations. Water binding sites and energies in $RNH_3^+ \cdot (H_2O)_n$ were examined as a function of $n$ and as a function of the nature of the R-group. R-groups ranged from simple alkyls to amide containing groups potentially able to form hydrogen bonds to the ammonium group. Effects of interest such as location and number of amide ≻C=O groups in R and the effect of size of R were investigated on carefully chosen molecules including alkylamines and lysine based systems, such as $CH_3(CH_2)_xNH_2$ ($x = 0$ and 9); acetylated lysine; and lysine containing peptides Ac–AAKAA and Ac–$A_x$K (Ac = acetyl, A = alanine, K = lysine; $x = 4$, 6, 8). For ammonium groups without intramolecular hydrogen bonds it was found that three water molecules form hydrogen bonds to the three hydrogen atoms of the ammonium group filling the first solvation shell. The fourth and fifth water molecules add to water of the first solvation shell (alkylamines) or at a charge-remote site (peptides). Water binding energies in $CH_3NH_3^+ \cdot (H_2O)_n$ steadily decrease with increasing $n$ (17, 14, 12, and 10 kcal/mol for $n = 1$, 2, 3, and 4, respectively) due to increasing charge delocalization over the bound $n - 1$ water molecules, thereby obscuring the start of a new solvation shell at $n = 4$. A simple electrostatic model, based on natural bond analysis (NBO) derived atomic charges, reproduces this effect quantitatively. Hydration of systems $RNH_3^+ \cdot (H_2O)_n$ with $m = 1$, 2, or 3 intramolecular hydrogen bonds is analogous to comparable systems $R'NH_3^+ \cdot (H_2O)_{n+m}$ with no intramolecular hydrogen bonds. For instance, theory indicates that lysine, when *N*-acetylated on either one of the two amines, exhibits one strong intramolecular hydrogen bond. In these systems the $RNH_3^+ \cdot (H_2O)_n \cdots H_2O$ binding energies are comparable to those of alkyl–$NH_3^+ \cdot (H_2O)_{n+1} \cdots H_2O$ and NBO calculations confirm that intramolecular hydrogen bonds remove a similar amount of charge from the ammonium group as intermolecular hydrogen bonds. The pentapeptide $(Ac–AAKAA)H^+$ was found to be a system with two intramolecular hydrogen bonds; the polypeptides $(Ac–A_xK)H^+$ ($x = 4$, 6, and 8) are systems with a fully self-solvated ammonium group. The binding energy of either charge-remote water or of water in a second solvation shell is ≤10 kcal/mol. Larger values occur for smaller systems, e.g., for $CH_3NH_3^+ \cdot (H_2O)_3 + H_2O$ $\Delta H^\circ = -10$ kcal/mol, and smaller values occur for larger systems, e.g., for $(Ac–A_8K)H^+ + H_2O$ $\Delta H^\circ = -5$ kcal/mol. A strong energy–entropy correlation of $\Delta S_n^\circ/\Delta H_n^\circ = 0.0018\,K^{-1}$ was experimentally found to hold for all hydration processes studied here.


*Keywords:* Peptide; Solvation shell; Ion mobility; van't Hoff analysis; Natural bond orbital analysis; Water binding energy

## 1. Introduction

Many salts readily dissolve in water not only for entropic reasons, but also because the energy required to disrupt the crystalline structure is significantly offset by the ion–water interaction, which is unusually strong due to the large dipole moment of water. Hence, water is most frequently the solvent of choice to pursue solution-phase ion chemistry. But because the ion–water interaction is so strong, it is often difficult to distinguish between effects caused by the solute and those caused by solute–solvent interaction. For instance, the ionic mobility (derived from the ionic conductivity) of the lithium ion in liquid water is smaller than that of the potassium ion [1], not because the lithium ion is larger than potassium but because lithium interacts more strongly with water. For polyatomic ions the question arises whether the ion geometry is an intrinsic property of the ion or whether it is largely determined by interactions with water. This question can be addressed by a comparison of

* Corresponding author. Tel.: +1 805 893 2893; fax: +1 805 893 8703.
*E-mail address:* bowers@chem.ucsb.edu (M.T. Bowers).

1387-3806/$ – see front matter © 2004 Elsevier B.V. All rights reserved.
doi:10.1016/j.ijms.2004.05.013

the solution- and gas-phase structures. For example, amino acids are known to be zwitterions in aqueous solution. In the gas phase, however, amino acids are not zwitterions, which has been shown in a number of experimental and theoretical studies [2]. Hence, amino acid zwitterions are only stable in solution because of favorable solute–solvent interactions.

The relative energy of different conformations of biological molecules (e.g., native state versus unfolded state) is in most cases expected to be dependent on the presence or absence of solvent and on the type of solvent. For instance, NMR-data obtained from aqueous solutions indicate that the Alzheimer's amyloid β-peptide (Aβ-peptide) is collapsed into a compact series of loops, strands, and turns without α-helical or β-sheet structure and with a fairly well defined hydrophobic core [3]. However, NMR-data taken in apolar solvents suggest that the Aβ-peptide is >50% (possibly as much as 82%) α-helical [4]. Gas-phase studies including ion mobility measurements and replica-exchange based molecular dynamics calculations indicate that the (free energy) preferred gas-phase structure of the Aβ-peptide is more compact than the structure in water and much more compact than the α-helical structure (Baumketner et al., unpublished results). Molecular mechanics results indicate that the compact gas-phase structures are "inside-out" structures defined by a network of strong electrostatic interactions (including salt bridges) in the core of the peptide (Baumketner et al., unpublished results).

These examples demonstrate clearly that the intrinsic (solvent-free) properties of an ion or polar molecule can be very different from those observed in aqueous solution. Hence, it is of paramount importance to understand the effects of hydration on the solute molecule on a molecular level. A promising approach to achieve this goal is to hydrate the solute molecule by adding water molecules one by one. This can be done by studying solute–water clusters composed of one solute molecule and a varying number of water molecules in the gas phase.

A very successful example of this approach are gas-phase equilibrium measurements involving water and small ions, which have provided a wealth of data on ion–water interactions [5]. With the development of soft ionization techniques such as matrix-assisted laser desorption ionization (MALDI) [6] and electrospray ionization (ESI) [7] to transfer large molecules into the gas phase sequential addition of water molecules can now be studied for biomolecules. ESI initiated equilibrium experiments have been carried out by a number of groups to study hydration of polyatomic ions such as organic amines, peptides, and even proteins [8–12]. One of the major findings of these studies is that the number of ionic groups on the molecule ("charge state") has a tremendous influence on the number of water molecules that cluster to the solute molecule under given experimental equilibrium conditions [11]. Hence, understanding the solvation of the ionic groups in a biomolecule is of particular interest.

In our laboratory, we have systematically studied the hydration of some of the ionic groups relevant for peptides and proteins: the ammonium, the guanidinium, and the carboxylate group. Some of the work has previously been published [11,13]. Here we focus on hydration of the ammonium group. We attempt to understand in detail the interaction between the ammonium group and each individual water molecule that is sequentially added, and we investigate how intramolecular hydrogen bonds to the ammonium group affect these water–ammonium interactions.

## 2. Experimental section

All experimental data were obtained using an electrospray mass spectrometer, which has previously been described in detail [14]. Briefly, the ions were produced in an electrospray ionization source, transported into a high-vacuum chamber via an ion funnel, and injected into a drift cell filled with either ~0.1–2.0 Torr of water vapor (hydration experiments) or 5 Torr helium (cross-section experiments). The drift cell is 4 cm in length and can be cooled by a flow liquid nitrogen or heated by electrical heaters. Ions drift through the cell under the influence of a weak uniform electric field provided by a series of equally spaced guard rings inside the cell. Ions leaving the drift cell through a small aperture are analyzed by a quadrupole mass filter and detected.

For the present study, two types of experiments were carried out on the same instrument: ion cross-section measurements in helium and equilibrium hydration measurements. For cross-section measurements the ion funnel is used to convert the continuous ion beam produced by ESI into an ion pulse [14], which is then injected into the drift cell filled with helium. By measuring the drift time $t_D$ of the ions their cross-section $\sigma$ can be determined using Eq. (1),

$$\sigma = \frac{3eV}{16NL^2}\left(\frac{2\pi}{\mu k_B T}\right)^{1/2} t_D \quad (1)$$

where $e$ is the ion charge, $V$ the drift voltage, $N$ the helium number density, $L$ the drift length, $\mu$ the reduced helium–ion mass, $k_B$ the Boltzmann constant, and $T$ the temperature [15].

In the equilibrium experiments ions are continuously injected into the drift cell filled with pure water vapor. Ions drifting through the cell are hydrated and quickly reach an equilibrium distribution of hydrated species $(M + H)^+ \cdot (H_2O)_n$. The distribution of $n$-values is analyzed by means of mass spectrometry in the quadrupole mass filter following the drift cell. Mass spectra obtained at different drift times (1–2 ms) were found to be identical, confirming that equilibrium is established inside the cell under the conditions used. Since the intensity $I_n$ of the $(M+H)^+ \cdot (H_2O)_n$ peak is proportional to the ion concentration $[(M+H)^+ \cdot (H_2O)_n]$, the ratio $I_n/I_{n-1}$ yields the equilibrium constant $K_n$ (Eq. (2)) for the equilibrium given in Eq. (3).

$$K_n = \frac{I_n}{I_{n-1}} \frac{760\,\text{Torr}}{P(H_2O)} \quad (2)$$

$$(M + H)^+ \cdot (H_2O)_{n-1} + H_2O \rightleftarrows (M + H)^+ \cdot (H_2O)_n \quad (3)$$

$P(H_2O)$ in Eq. (2) is the measured water pressure. For a series of measurements at constant temperature but variable pressure the equilibrium constant $K_n$ is obtained from the slope of a plot of $I_n/I_{n-1}$ versus pressure. Repeating this procedure at various temperatures yields the temperature dependence of $K_n$ and hence $\Delta G_n^\circ$ (Eq. (4)).

$$\Delta G_n^\circ = -RT \ln K_n \quad (4)$$

$$\Delta G_n^\circ = \Delta H_n^\circ - T\Delta S_n^\circ \quad (5)$$

From a plot of $\Delta G_n^\circ$ versus $T$ (Eq. (5)), values for $\Delta H_n^\circ$ and $\Delta S_n^\circ$ are obtained from the intercept and the slope of a straight line through the data, respectively.

## 3. Theory

In an attempt to theoretically understand experimental trends, hydration was also studied by computer simulations using molecular mechanics/molecular dynamics (MM/MD) and density functional theory (DFT) methods. MM/MD was used to generate model structures by a simulated annealing protocol identical to that previously used [16]. These calculations employ the AMBER suit of programs together with the standard AMBER force field to generate at least a hundred candidate structures [17]. For the water molecule the TIP3P model [18] is used with modified charges of +0.329 on hydrogen and −0.658 on oxygen (Kollman, private communication) to account for the gas-phase water dipole moment of 1.85 D [1]. The set of MM-structures is analyzed in terms of energy and cross-section for comparison with experiment where available. Orientation-averaged projection cross-sections are obtained using atomic collision radii parameterized to account for the ion–helium interaction potential [19]. For the molecules of this study it is found that the lowest energy structure located in each system is a typical representative of the entire family of low energy structures. Hence, the lowest energy structures were chosen for figures, numbers in tables, and in selected cases for further analysis by higher level theory including DFT-based Natural Bond Orbital (NBO) analysis calculations using the unrestricted open shell B3LYP functional [20,21] and a 6−311++G** basis set as implemented in the GAUSSIAN98 software package [22].

## 4. Results and discussion

Protonated primary alkylamines are a good choice for studying hydration of the free $–NH_3^+$ group with a minimum of interference by other functional groups in the molecule. Experimental and theoretical water binding energies reported in the literature for protonated *n*-alkyl amines are compiled in Table 1. Interestingly, all experimental studies agree that the first water molecule is most strongly bound, and that each additional water molecule is less strongly bound (by 15–20%) than the previous one. At first glance this is not necessarily expected. Model structures show that more than one H-bond to $–NH_3^+$ per water molecule is not feasible even for the first water [11]. Hence, for a free protonated primary amine (i.e., not engaged in any intramolecular hydrogen bonds) it could be argued that the first three water molecules are expected to bind about equally strongly, because each water molecule has the opportunity to form the same type of hydrogen bond with one of the three amine hydrogens in $–NH_3^+$. Model structures also indicate that there is no steric interference between three waters around a protonated amine [11]. Yet both experiment and DFT theory indicate that the water binding energy is steadily decreasing from the first through the third water molecule [10,11,23,24].

A second interesting observation is that the decrease from the third to fourth water molecule follows the same trend established by the first three waters. The start of a new hydration shell by the fourth water molecule is not reflected in the binding energies. This is even true for DFT calculations where we know for a fact that the fourth water molecule is indeed in the second solvation shell [11]. On the other hand, binding energies obtained by a molecular mechanics approach (AMBER) show a clear solvation shell pattern:

Table 1
Experimental and theoretical water binding energies (kcal/mol) reported in the literature for the first through fifth water molecule adding to protonated primary *n*-alkylamines

| | | 1 | 2 | 3 | 4 | 5 | Reference |
|---|---|---|---|---|---|---|---|
| $CH_3NH_3^+$ | Experiment | 18.8 | 14.6 | 12.4 | | | [23] |
| | Experiment | 16.8 | 14.6 | 12.3 | 10.3 | | [24] |
| | DFT | 16.9 | 13.9 | 11.9 | 9.3 | | [11] |
| $C_2H_5NH_3^+$ | Experiment | 17.5 | 14.7 | 13.2 | | | [23] |
| *n*-$C_3H_7NH_3^+$ | Experiment | 15.1 | 11.6 | 10.3 | 9.9 | | [24] |
| | Experiment | 15.6 | | | | | [10] |
| *n*-$C_6H_{13}NH_3^+$ | Experiment | 15.2 | | | | | [10] |
| *n*-$C_{10}H_{21}NH_3^+$ | Experiment | 14.8 | 12.1 | 9.6 | 7.5 | 6.7 | [11] |
| | MM | 13.9 | 12.6 | 11.4 | 7.8 | 7.7 | [11] |

the first three water molecules have similar binding energies (11.4–13.9 kcal/mol), the following water molecules in the second solvation shell are substantially less strongly bound (<8 kcal/mol) [11].

The DFT and experimental findings can qualitatively be rationalized by a partial delocalization of the charge on the $–NH_3^+$ group over the associated water molecules. The more water molecules ligated the more the charge is delocalized. Hence, the electrostatic interactions with successively ligated water molecules are successively weaker. In molecular mechanics calculations, on the other hand, the point charge on each atom is kept constant. Therefore, charge delocalization never occurs and as a result a solvation shell pattern is observed for the binding energies.

In order to obtain quantitative information on charge delocalization we performed NBO calculations on protonated methylamine with zero through four water molecules added, using the same level of theory as employed for the water binding energy calculations in Table 1 [11]. On the basis of simple electrostatics these calculations provide a tool to test whether the amount of charge delocalization can account for the water binding energy pattern observed. Table 2 lists the NBO charges on all of the atoms of interest. It can be seen that the negative charge on N changes from −0.672 for non-hydrated $CH_3–NH_3^+$ to −0.750 for the quadruply hydrated molecule. Similarly, the positive charge on amino hydrogens not engaged in a hydrogen bond decreases from +0.442 (no water) to +0.414 (two waters). The overall decrease of charge on the amino group is compensated for by an increase of the charge on the water molecule(s) added: +0.048 (one water), +0.076 (two waters), +0.096 (three waters), +0.102 (four waters). Hence, the trend in the NBO charge distribution agrees qualitatively very nicely with the decrease of water binding energies as a function of water addition.

For a quantitative comparison with water binding energies the NBO charge distributions are converted to energies using Coulomb's law. For simplicity the charge distribution spread over an orbital centered at a particular atom is treated as a point charge at the location of the atom, a simplification that will lead to an overestimation of Coulomb terms. Using these point charges the electrostatic contribution $E_{el}$ to the water binding energy is calculated as the sum of pair-wise point charge interactions between each atom of the water molecule added (atoms $i = 1$–3) and each of the remaining atoms ($j = 4$ through $8 + 3n$) in the $CH_3NH_3^+ \cdot (H_2O)_n$ system (Eq. (6))

$$E_{el} = -\sum_{i=1}^{3}\sum_{j=4}^{8+3n}\frac{q_i q_j}{r_{ij}} \quad (6)$$

where the point charges on atoms $i$ and $j$ separated by $r_{ij}$ are $q_i$ and $q_j$, respectively. Using the values in Table 2 for $q_i$ and $q_j$, we find the quantity $E_{el}$ decreases steadily as a function of $n$ as can be seen in Fig. 1 (× symbols), with the decrease in $E_{el}$ from $n$ to $n + 1$ comparable to the decrease

Table 2
NBO charges for bare and hydrated $CH_3NH_3^+$

| Atom | Molecule | | |
|---|---|---|---|
| | $CH_3NH_3^+$ | $H_2O$ | $CH_3NH_3^+ \cdot H_2O$ |
| N | −0.672 | | −0.698 |
| $H_1$ | +0.442 | | +0.472[a] |
| $H_2$ | +0.442 | | +0.428 |
| $H_3$ | +0.442 | | +0.428 |
| $O_1$ | | −0.916 | −0.960 |
| $H_{a1}$ | | +0.458 | +0.504 |
| $H_{b1}$ | | +0.458 | +0.504 |

| Atom | Molecule | | |
|---|---|---|---|
| | $CH_3NH_3^+ \cdot (H_2O)_2$ | $CH_3NH_3^+ \cdot (H_2O)_3$ | $CH_3NH_3^+ \cdot (H_2O)_4$ |
| N | −0.722 | −0.746 | −0.750 |
| $H_1$ | +0.464[a] | +0.454 | +0.450[a] |
| $H_2$ | +0.464[b] | +0.454 | +0.450[b] |
| $H_3$ | +0.414 | +0.454 | +0.460[c] |
| $O_1$ | −0.958 | −0.956 | −0.956 |
| $H_{a1}$ | +0.498 | +0.494 | +0.492 |
| $H_{b1}$ | +0.498 | +0.494 | +0.492 |
| $O_2$ | −0.958 | −0.956 | −0.956 |
| $H_{a2}$ | +0.498 | +0.494 | +0.492 |
| $H_{b2}$ | +0.498 | +0.494 | +0.492 |
| $O_3$ | | −0.956 | −0.986 |
| $H_{a3}$ | | +0.494 | +0.486 |
| $H_{b3}$ | | +0.494 | +0.518[d] |
| $O_4$ | | | −0.952 |
| $H_{a4}$ | | | +0.490 |
| $H_{b4}$ | | | +0.490 |

[a] H-bond to $O_1$.
[b] H-bond to $O_2$.
[c] H-bond to $O_3$.
[d] H-bond to $O_4$.

observed in the experimental binding energies $-\Delta H_n^\circ$ (dots in Fig. 1). The absolute values of $E_{el}$ and $-\Delta H_n^\circ$ are offset from each other by 7 kcal/mol. However, quantitative agreement of absolute values is not expected for several reasons. First, the charge on the ammonium group of *n*-decylamine is

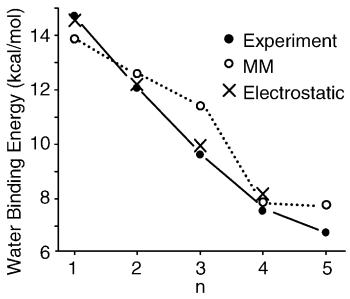


Fig. 1. Experimental (dots) and MM-based theoretical (circles) water binding energies for the first through fifth water molecule adding to *n*-decylamine. Also indicated is the trend of the electrostatic interaction (×) between the *n*th water molecule and the $(n - 1)$th *n*-decylamine hydrate based on $CH_3NH_3^+$ NBO-charges (the scale of the electrostatic interaction is reduced by 7.0 kcal/mol; see text).

Table 3
Measured and calculated collision cross-sections

| | Cross-section (Å$^2$) | |
|---|---|---|
| | Measured[a] | Calculated[b] |
| *N*ε-Ac–Lys[c] | 79 | 81 |
| *N*α-Ac–Lys[d] | 79 | 79 |
| *N*α-Ac–Lys–OMe[e] | 85 | 85 |
| Ac–AAKAA | 146 | 148 |
| Ac–AAAAK | 148 | 146 |
| Ac–AAAAAAK | 178 | 180 |
| Ac–AAAAAAAAK | 209 | 210 |

[a] Cross-section determined at 300 K. Error ±2%.
[b] See Section 3.
[c] *N*ε-Acetyllysine (see footnote 1).
[d] *N*α-Acetyllysine (see footnote 2).
[e] *N*α-Acetyllysine methyl ester.

expected to be smaller than that of methylamine because the large alkyl group provides increased intramolecular charge delocalization (refer to Table 1). Second, electrostatics is not the only factor contributing to the water binding energy. And third, the point charge approximation in the model is rather poor yielding a model water dipole moment of 2.58 D, a factor of 1.4 too high. Nevertheless, the electrostatic model reproduces the experimental *trend* very nicely and therefore offers a reasonable explanation for why the water binding energy steadily decreases with water addition and why the start of a new solvation shell at the fourth water molecule is not reflected in a significant decrease of $-\Delta H_4^\circ$ compared to $-\Delta H_3^\circ$.

For peptides and proteins the situation is somewhat more complex because these molecules provide at least one intramolecular hydrogen bond acceptor (backbone >C=O) per residue that potentially competes with water for solvating protonated amines. Molecular modeling results indicate that the protonated N-terminus of very short peptides (two or three residues) cannot efficiently be solvated by the backbone carbonyl groups for steric reasons [11,25]. Much better self-solvation can be achieved by flexible side chains with electron-rich functional groups. *N*ε-acetyllysine[1] is an example where the side chain carbonyl oxygen forms a perfect intramolecular hydrogen bond with the protonated N-terminus (Fig. 2a). Good charge solvation can also be achieved in *N*α-acetyllysine[2] and its methyl ester with the protonated side chain amino group solvated by the carbonyl of the *N*α-acetyl group (Fig. 2b and c). Note, that although the structures shown in Fig. 2 are based on a low level theoretical approach (MM potential search with subsequent DFT optimization), they are in very good agreement with experimental cross-section data (Table 3) and therefore very plausible.

The experimental water binding energies of the three derivatized lysine systems, summarized in Table 4, indi-

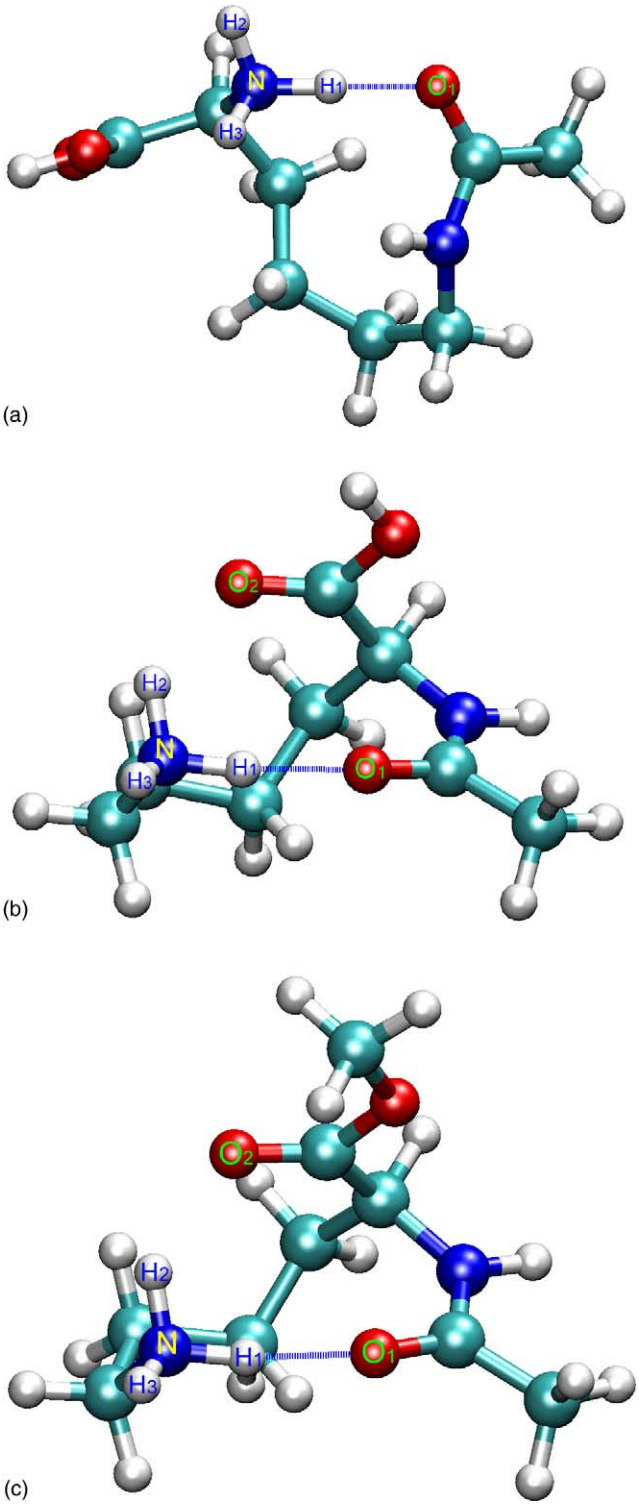


Fig. 2. Molecular structure of protonated (a) *N*ε-acetyllysine (see footnote 1), (b) *N*α-acetyllysine (see footnote 2), and (c) *N*α-acetyllysine methyl ester obtained by molecular mechanics and subsequent DFT-optimization. Shown as a blue dashed line is the strong intramolecular hydrogen bond between the ammonium group and the acetamide oxygen atom.

[1] Lysine with acetylated amino group in ϵ-position (side chain).
[2] Lysine with acetylated amino group in α-position.

Table 4
Theoretical binding energies[a] $E_n$ and experimental $\Delta H_n^\circ$ and $\Delta S_n^\circ$ values for the sequential ($n-1 \rightarrow n$) hydration of the protonated species indicated

| | $n$ | $E_n$ (kcal/mol) | $-\Delta H_n^\circ$ (kcal/mol) | $-\Delta S_n^\circ$ (cal/(mol K)) |
|---|---|---|---|---|
| *N*ε-Ac–Lys[b,c] | 1 | 11.2 | 10.1 | 16.7 |
| | 2 | 10.4 | 8.9 | 16.0 |
| | 3 | 10.0 | 7.7 | 15.9 |
| *N*α-Ac–Lys[b,d] | 1 | 12.0 | 10.6 | 17.6 |
| | 2 | 9.6 | 8.4 | 14.6 |
| | 3 | 9.7 | 8.3 | 16.7 |
| | 4 | 6.4 | 7.2 | 14.7 |
| *N*α-Ac–Lys–OMe[b,e] | 1 | 10.7 | 10.4 | 17.8 |
| | 2 | 8.9 | 7.8 | 13.5 |
| | 3 | 8.5 | 7.1 | 13.7 |
| Ac–AAKAA[f] | 1 | 11.5 | 8.5 | 17.9 |
| | 2 | 9.7 | 7.4 | 13.9 |
| Ac–AAAAK[f] | 1 | 10.4 | 6.9 | 13.5 |

[a] Obtained by molecular mechanics (AMBER).
[b] Error levels are ±0.3 kcal/mol for $\Delta H_n^\circ$ and ±1 cal/(mol K) for $\Delta S_n^\circ$.
[c] *N*ε-Acetyllysine (see footnote 1).
[d] *N*α-Acetyllysine (see footnote 2).
[e] *N*α-Acetyllysine methyl ester.
[f] Error levels are ±0.7 kcal/mol for $\Delta H_n^\circ$ and ±2 cal/(mol K) for $\Delta S_n^\circ$.

Table 5
NBO charges on selected atoms of protonated acetyllysine systems

| Atom[a] | Molecule | | |
|---|---|---|---|
| | *N*ε-Ac–Lys (Fig. 2a) | *N*α-Ac–Lys (Fig. 2b) | *N*α-Ac–Lys–OMe (Fig. 2c) |
| N | −0.725 | −0.718 | −0.720 |
| $H_1$ | +0.463[b] | +0.472[b] | +0.472[b] |
| $H_2$ | +0.430 | +0.446[c] | +0.449[c] |
| $H_3$ | +0.431 | +0.419 | +0.417 |
| $O_1$ | −0.698 | −0.730 | −0.731 |
| $O_2$ | −0.533 | −0.652 | −0.663 |

[a] N, $H_1$, $H_2$, and $H_3$ are atoms of the ammonium group; $O_1$ is carbonyl oxygen of amide; $O_2$ is carbonyl oxygen of carboxylic acid/ester.
[b] Intramolecular H-bond with acetyl carbonyl oxygen.
[c] Intramolecular interaction with C-terminus carbonyl oxygen.

cate that the intramolecular hydrogen bond weakens the water–ammonium interaction. This effect can be rationalized by the same argument used above. Part of the positive charge on the protonated amine is transferred to the intramolecular H-bond acceptor thereby decreasing the electrostatic interaction between the ammonium group and water. An NBO-analysis on these derivatized lysine systems demonstrates this effect very clearly (Table 5). The ammonium nitrogens with an internal H-bond are more negative (−0.72) compared to free amines (−0.67) and the hydrogens less positive (see Tables 2 and 5). It could be argued that the intramolecular H-bond in the lysine systems assumes the charge solvating power of the intermolecular H-bond in alkyl–$NH_3^+ \cdot H_2O$. This is supported by the experimental hydration enthalpies compiled in Tables 1 and 4, which indicate that $\Delta H_n^\circ$ of the lysine systems are roughly equivalent to $\Delta H_{n+1}^\circ$ of $C_{10}H_{21}NH_3^+$.

The functional group providing intramolecular charge solvation in all three lysine systems shown in Fig. 2 is the carboxyl amide > C=O group. The carboxylic acid and ester > C=O groups, also present in all three systems, are less favorable for charge solvation because of steric considerations (particularly important in *N*ε-acetyllysine, Fig. 2a) and for electrostatic reasons. The NBO calculations summarized in Table 5 provide quantitative information for the qualitative effect[3] that carboxyl amide oxygens are more negative than their carboxylic acid counter parts (by 0.08–0.16 charge units).

Model structures of $C_{10}H_{21}NH_3^+ \cdot (H_2O)_7$ indicate that the seven water molecules form a water cluster around the –$NH_3^+$-group [11]. For peptides the situation is different. Water molecules like to bind in charge-remote locations if the charge is already solvated by a first solvation shell of intra- or intermolecular interactions. For instance, in

[3] For example, the dipole moment of acetamide is 3.7 D, that of acetic acid 1.7 D. See Ref. [1].

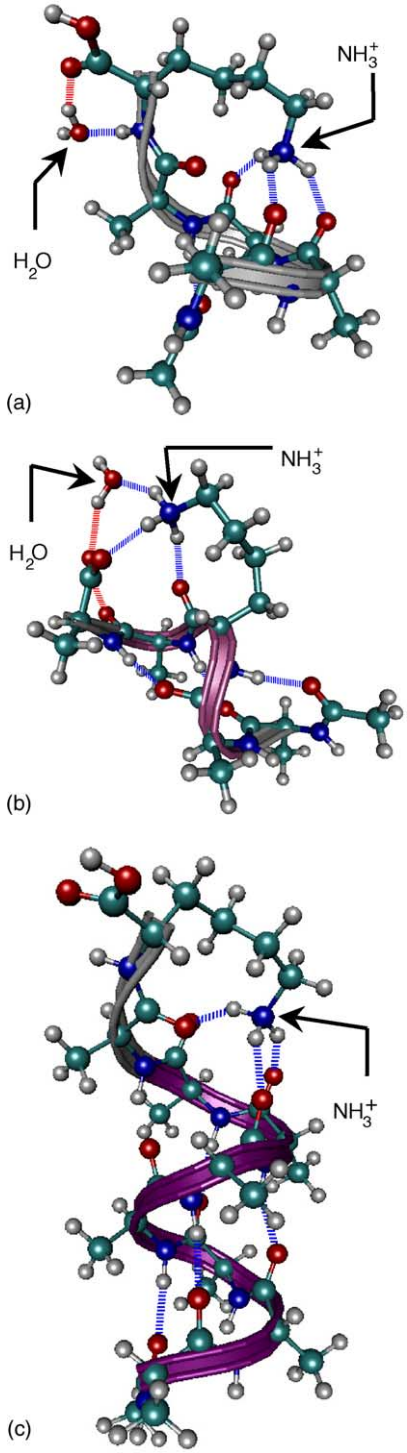


Fig. 3. Molecular mechanics structures of (a) (Ac–$A_4$K)$H^+$·$H_2O$, (b) (Ac–AAKAA)$H^+$·$H_2O$, and (c) (Ac–$A_8$K)$H^+$.

protonated dialanine hydrated by five water molecules, $(AA)H^+ \cdot (H_2O)_5$, the charge-remote C-terminus is a preferred binding site [11]. In this system the ammonium group is fully solvated by the intermolecular interactions with three water molecules. Similarly, AMBER molecular modeling results indicate that the acetylated and protonated pentapeptide (Ac–AAAAK)$H^+$ is a system where the lysine ammonium group is fully solvated by three intramolecular H-bond acceptors (backbone carbonyls) and provides another example where theory predicts charge-remote water addition (Fig. 3a). The comparatively small experimental (Ac–AAAAK)$H^+ \cdots H_2O$ binding energy of 6.9 kcal/mol (Table 4) provides support for the theoretical result. For the (Ac–AAKAA)$H^+$ system of identical size the water binding energy is measured to be 8.5 kcal/mol. In this system theory indicates that the lysine ammonium group is involved in only two intramolecular H-bonds and that the water molecule adds directly to the charged –$NH_3^+$-group (Fig. 3b).

The structures for singly hydrated (Ac–AAAAK)$H^+$ and (Ac–AAKAA)$H^+$ shown in Fig. 3a and b are distinctly different. The structure for (Ac–AAKAA)$H^+$, where lysine is placed in the middle position, is a random coil providing only partial self-solvation of the charge. The molecule with lysine at the C-terminus, however, folds into a structure directly analogous to the C-terminal end of the α-helix found in longer homologous peptides (Ac–$A_8$K)$H^+$ (Fig. 3c) and (Ac–$A_{20}$K)$H^+$ [9,26]. In the helical structures, confirmed by cross-section measurements (Table 3 and Ref. [9]), the three dangling backbone ≻C=O hydrogen bond acceptors are nicely capped by the lysine side chain. In addition, the positive charge on lysine lines up favorably with the helix dipole. Hence, the homologous series of structurally related (Ac–$A_x$K)$H^+$ peptides provides an opportunity to study the effect of system size on the water binding energy for charge remote binding. Hydration mass spectra shown in Fig. 4a–c indicate that water addition becomes increasingly more difficult with increasing system size. In contrast to the smaller (Ac–$A_4$K)$H^+$ system, both of the larger (Ac–$A_6$K)$H^+$ and (Ac–$A_8$K)$H^+$ molecules stay preferentially dehydrated even under the most favorable experimental conditions (260 K, 1.3 Torr water vapor) making accurate measurements of $\Delta H_n^\circ$ and $\Delta S_n^\circ$ of hydration impossible. However, $\Delta G_1^\circ$-values obtained at 260 K are listed in Table 6 along with estimated $\Delta H_1^\circ$-values demonstrating the significant decrease in the water binding energy with increasing system size.

A possible explanation for this trend is that electrostatic interactions between the water dipole and the charged peptide are still important even for charge remote water binding

Table 6
Experimental Gibbs free energy and enthalpy changes for the addition of one water molecule to the peptides (Ac–$A_x$K)$H^+$

| $x$ | $-\Delta G_1^\circ$ (260 K) | $-\Delta H_1^\circ$ |
|---|---|---|
| 4 | 3.4 | 6.9 |
| 6 | 3.1 | 5.8[b] |
| 8 | 2.6 | 4.9[b] |
| 20 | <2.3[a] | <4.3[b] |

[a] Estimated using $-\Delta G_1^\circ$ (243 K) <2.5 kcal/mol [26]; $-\Delta G_1^\circ$ (260 K) ≅ $-\Delta G_1^\circ$ (243 K) − 17 K × $\Delta S_1^\circ$; and $\Delta S_1^\circ \cong -13$ cal/(mol K) (Table 4).
[b] Estimated using $-\Delta G_1^\circ$ (260 K) and Eq. (7).

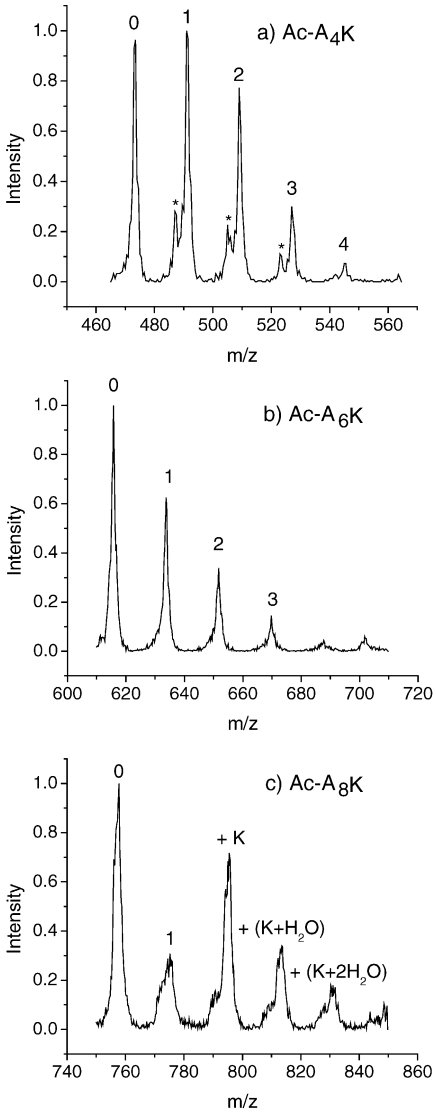


Fig. 4. Mass spectra of Ac–$A_x$K (a) $x = 4$, (b) $x = 6$, and (c) $x = 8$ recorded after passing the ion beam through the drift cell filled with 1.3 Torr of water vapor at 260 K. Numbers above the peaks indicate the number of water molecules added to the protonated species. Peaks due to impurities are labeled with an asterisk (*). The Ac–$A_8$K spectrum (c) shows intense peaks corresponding to potassiated species.

sites. Molecular mechanics simulations provide support for this possibility: the preferred water binding sites are found to be on the C-terminal side of the molecule in relatively close proximity to the charge (Fig. 3a and Ref. [26]). With increasing peptide size the helix dipole moment becomes increasingly larger as the positive end of the helix dipole (located on the N-terminus) is moved away from the positive lysine residue (located at the C-terminus). Hence, increasing the space between N- and C-termini moves part of the positive charge farther away from the C-terminus where the water is preferentially bound and consequently reduces the electrostatic contribution to the water−peptide interaction energy.

The equilibrium experiments carried out for this study not only yield energetic but also entropic information about

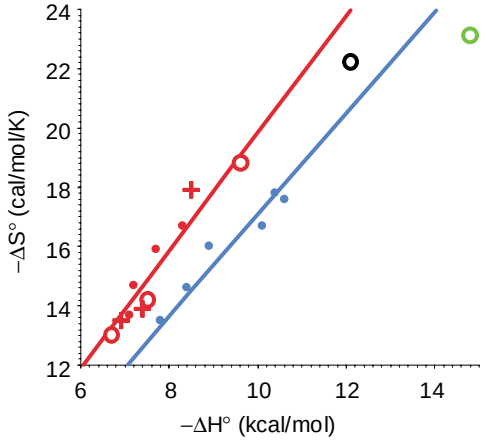


Fig. 5. Plot of entropy versus enthalpy of hydration measured experimentally for the protonated species of *n*-decylamine (open circles), acetyllysine systems (red and blue dots), and the acetylated pentapeptides Ac–AAKAA and Ac–AAAAK (+ symbol). Data with above average $\Delta S_n^\circ/\Delta H_n^\circ$ ratio are red, data below average blue, data in between black, and data much below average green. The red and blue lines are linear regressions through the origin and the data of the same color.

hydration. Fig. 5 shows a plot of $\Delta S_n^\circ$ values versus the corresponding $\Delta H_n^\circ$ values for all the systems included in this study. It is evident that there is a strong correlation between the change of entropy and the change of enthalpy upon addition of a water molecule to any system, which can be quantified by Eq. (7).

$$\Delta S_n^\circ = \frac{1.8 \pm 0.2}{1000\,\mathrm{K}} \Delta H_n^\circ \tag{7}$$

This correlation is not surprising, because a tightly bound water molecule gives rise to both a large binding energy and a large loss of entropy. However, there are systematic deviations from the linear correlation. The data shown in Fig. 5 can be grouped into data with above average (red) and below average (blue) $\Delta S_n^\circ/\Delta H_n^\circ$ ratio.

A closer examination of the *n*-decylamine data [11], shown as circles in Fig. 5, indicates that the entropy loss upon addition of the first water molecule (green circle) is rather small compared to the large binding energy, suggesting that the $C_{10}H_{22}NH_3^+ \cdot H_2O$ complex is relatively floppy. The $\Delta S_n^\circ/\Delta H_n^\circ$ ratio for the second water molecule (black circle) is about average, whereas the data for the third, fourth, and fifth water (red circles) are part of the red data set with large $\Delta S_n^\circ$ values. A similar trend is observed for the derivatized lysine systems (dots), *N*α-acetyllysine, *N*α-acetyllysine methyl ester, and *N*ε-acetyllysine. For all three systems addition of the first and second water molecule yields below average $\Delta S_n^\circ/\Delta H_n^\circ$ ratios (blue dots), addition of the third and fourth water yields ratios above average (red dots). The (Ac–AAAAK)$H^+$ and (Ac–AAKAA)$H^+$ systems with more extensive self-solvation of the charge (red crosses) form water clusters with relatively little flexibility (large $\Delta S_n^\circ/\Delta H_n^\circ$ ratios).

Hence, the entropy data suggest that there is a correlation between $\Delta S_n^\circ/\Delta H_n^\circ$ ratio and the degree of charge

solvation (intra- and/or intermolecular). Water addition to systems with no or single solvation of the $–NH_3^+$ group yield data belonging to the blue set (relatively floppy hydrates), whereas addition of water to systems with a filled first solvation shell around the $–NH_3^+$ group belong to the red data set (relatively rigid hydrates). The exact location of the switch from red to blue appears to be system dependent.

## 5. Conclusions

In this work we examined the hydration of a variety of protonated amines. The issues include the effect of existing intramolecular hydrogen bonds on both structural and energetic aspects of water addition; the effect of prior water addition on new water addition; and the competition between charge proximate and charge remote water addition sites. We arrive at the following conclusions.

1. Sequential hydration energies of a number of protonated alkylamines, from $CH_3NH_3^+$ to $n$-$C_{10}H_{21}NH_3^+$ have been reported in the literature. These binding energies fall off in a gradual manner with no indication a first solvation shell fills and a second is initiated. Theoretical work (DFT and MM/MD) reported here indicates a first solvation sphere of three waters (one bonding to each H-center on $–NH_3^+$) with subsequent water molecules bonding to other water molecules only. DFT calculations yield water-binding trends in agreement with experiment where no shell filling drop-off is observed.
2. The experimental trend in hydration energies is quantitatively fit using an electrostatic model and atomic charges on the $–NH_3^+$ group and attached water molecules calculated using an NBO analysis. No shell filling drop-off is predicted.
3. MM calculations give good agreement with absolute hydration energies but show a definite shell-filling effect. This occurs because the charges on all atoms are independent of the degree of hydration whereas DFT calculations naturally incorporate these changes.
4. In *N*-acetyllysines the protonated amino group is predicted to have one intramolecular H-bond and a shell filling on addition of two water molecules. The measured binding energies of these molecules is comparable to addition of the second and third water molecules to comparable sized alkylamines (free $–NH_3^+$ group), in support of the theoretical prediction.
5. In the protonated pentapeptides $(Ac–AAKAA)H^+$ and $(Ac–AAAAK)H^+$ the amino group on the lysine has two and three intramolecular hydrogen bonds, respectively, according to MM calculations. The measured hydration energies are 8.5 and 6.9 kcal/mol, respectively, for adding the first water molecule in support of theory.
6. Experimental cross-sections for all peptides considered here are in excellent agreement with theoretical cross-sections, supporting the theoretical structures used in analyzing the hydration data.
7. Water binding becomes dramatically weaker as chain length increases in the helical peptides $(Ac–A_xK)H^+$. The apparent cause is the increased separation of charge (i.e., increased helix dipole) as chain length increases destabilizing addition of water.
8. Experiment indicates a strong entropy/enthalpy of hydration correlation that subtly varies with degree of hydration. An approximate ratio of $\Delta S_n^\circ/\Delta H_n^\circ$ of $0.0018\,K^{-1}$ is found for the systems studied here.

## Acknowledgements

Dr. Catherine J. Carpenter's help for editing this paper is highly appreciated. The support of the National Science Foundation under grant CHE-0140215 is gratefully acknowledged.

## References

[1] D.R. Lide (Ed.), CRC Handbook of Chemistry and Physic, 84th ed., CRC, Boca Raton, FL, 2003. http://www.hbcpnetbase.com.
[2] See e.g.: (a) R.D. Suenham, F.J. Lovas, J. Mol. Spectrosc. 72 (1978) 372;
(b) R.D. Brown, P.D. Godfrey, J.W.V. Storey, M.-P. Bassez, J. Chem. Soc., Chem. Commun. 13 (1978) 547;
(c) C.J. Chapo, J.B. Paul, R.A. Provencal, K. Roth, R.J. Saykally, J. Am. Chem. Soc. 120 (1998) 12956;
(d) J.H. Jensen, M.S. Gordon, J. Am. Chem. Soc. 117 (1995) 8159.
[3] Structural conclusions for the full-length peptide Aβ(1–42) are based on NMR-data of Aβ(10–35) and Aβ(1–40), which are claimed to be paradigmatic for the hydrophobic core region of Aβ(1–42). S. Zhang, K. Iwata, M.J. Lachenmann, J.W. Peng, S. Li, E.R. Stimson, Y.-A. Lu, A.M. Felix, J.E. Maggio, J.P. Lee, J. Struct. Biol. 130 (2000) 130.
[4] O. Crescenzi, S. Tomaselli, R. Guerrini, S. Salvadori, A.M. D'Ursi, P.A. Temussi, D. Picone, Eur. J. Biochem. 269 (2002) 5642.
[5] See, for example: R.G. Keesee, A.W. Castleman Jr., J. Phys. Chem. Ref. Data 15 (1986) 1011.
[6] (a) M. Karas, F. Hillenkamp, Anal. Chem. 60 (1988) 2288;
(b) F. Hillenkamp, Adv. Mass Spectrom. 11 (1989) 354.
[7] J.B. Fenn, M. Mann, C.K. Meng, S.F. Wong, Science 246 (1989) 64.
[8] (a) J.S. Klassen, A.T. Blades, P. Kebarle, J. Phys. Chem. 99 (1995) 15509;
(b) J. Woenckhaus, Y. Mao, M.F. Jarrold, J. Phys. Chem. B 101 (1997) 847;
(c) J. Woenckhaus, R.R. Hudgins, M.F. Jarrold, J. Am. Chem. Soc. 119 (1997) 9586.
[9] M. Kohtani, M.F. Jarrold, J. Am. Chem. Soc. 124 (2002) 11148.
[10] A.T. Blades, J.S. Klassen, P. Kebarle, J. Am. Chem. Soc. 118 (1996) 12437.
[11] D. Liu, T. Wyttenbach, P.E. Barran, M.T. Bowers, J. Am. Chem. Soc. 125 (2003) 8458.
[12] T. Wyttenbach, B. Paizs, P.E. Barran, L. Breci, D. Liu, S. Suhai, V.H. Wysocki, M.T. Bowers, J. Am. Chem. Soc. 125 (2003) 13768.
[13] D. Liu, T. Wyttenbach, C.J. Carpenter, M.T. Bowers, J. Am. Chem. Soc. 126 (2004) 3261.

[14] T. Wyttenbach, P.R. Kemper, M.T. Bowers, Int. J. Mass Spectrom. 212 (2001) 13.
[15] E.A. Mason, E.W. McDaniel, Transport Properties of Ions in Gases, Wiley, New York, 1988.
[16] T. Wyttenbach, G.V. Helden, M.T. Bowers, J. Am. Chem. Soc. 118 (1996) 8355.
[17] D.A. Case, D.A. Pearlman, J.W. Caldwell, T.E. Cheatham III, J. Wang, W.S. Ross, C.L. Simmerling, T.A. Dearden, K.M. Merz, R.V. Stanton, A.L. Cheng, J.J. Vincent, M. Crowley, V. Tsui, H. Gohlke, R.J. Radmer, Y. Duan, J. Pittera, I. Massova, G.L. Seibel, U.C. Singh, P.K. Weiner, P.A. Kollman, AMBER 7, University of California, San Francisco, 2002.
[18] W.L. Jorgensen, J. Chandrasekhar, J.D. Madura, R.W. Impey, M.L. Klein, J. Chem. Phys. 79 (1983) 926.
[19] T. Wyttenbach, G. Von Helden, J.J. Batka, D. Carlat, M.T. Bowers, J. Am. Soc. Mass Spectrom. 8 (1997) 275.
[20] P.J. Stephens, F.J. Devlin, C.F. Chabalowski, M.J. Frisch, J. Phys. Chem. 98 (1994) 11623.
[21] A.D. Becke, J. Chem. Phys. 98 (1993) 5648.
[22] M.J. Frisch, G.W. Trucks, H.B. Schlegel, G.E. Scuseria, M.A. Robb, J.R. Cheeseman, V.G. Zakrzewski, J.A. Montgomery, R.E. Stratmann Jr., J.C. Burant, S. Dapprich, J.M. Millam, A.D. Daniels, K.N. Kudin, M.C. Strain, O. Farkas, J. Tomasi, V. Barone, M. Cossi, R. Cammi, B. Mennucci, C. Pomelli, C. Adamo, S. Clifford, J. Ochterski, G.A. Petersson, P.Y. Ayala, Q. Cui, K. Morokuma, D.K. Malick, A.D. Rabuck, K. Raghavachari, J.B. Foresman, J. Cioslowski, J.V. Ortiz, A.G. Baboul, B.B. Stefanov, G. Liu, A. Liashenko, P. Piskorz, I. Komaromi, R. Gomperts, R.L. Martin, D.J. Fox, T. Keith, M.A. Al-Laham, C.Y. Peng, A. Nanayakkara, C. Gonzalez, M. Challacombe, P.M.W. Gill, B. Johnson, W. Chen, M.W. Wong, J.L. Andres, C. Gonzalez, M. Head-Gordon, E.S. Replogle, J.A. Pople, Gaussian98, revision A.5, Gaussian, Inc., Pittsburgh, PA, 1998.
[23] Y.K. Lau, P. Kebarle, Can. J. Chem. 59 (1981) 151.
[24] M. Meot-Ner, J. Am. Chem. Soc. 106 (1984) 1265.
[25] S. Campbell, M.T. Rodgers, E.M. Marzluff, J.L. Beauchamp, J. Am. Chem. Soc. 117 (1995) 12840.
[26] R.R. Hudgins, M.F. Jarrold, J. Am. Chem. Soc. 121 (1999) 3494.